

Magnetohydrodynamic Flow Past a Permeable Bed

R. VENUGOPAL & D. BATHAIAH

Department of Mathematics, Sri Venkateswara University, Tirupati 517502

Received 16 May 1981

Abstract. The paper evaluates mass flow velocity heat transfer rates and velocity/temperature distributions in the viscous, incompressible and slightly conducting fluid past a permeable bed in three different configurations namely (1) Couette flow (2) Poiseuille flow and (3) free surface flow, under the influence of a uniform transverse magnetic field. To discuss the solution, the flow region is divided into two zones: Zone 1 (from the impermeable upper rigid plate to the permeable bed) in which the flow is laminar and governed by Navier-Stokes equations, and Zone 2 (the permeable bed below the nominal surface) in which the flow is governed by Darcy law. The paper also investigates the effects of magnetic field, porosity and Biot number on the physical quantities mentioned above.

1. Introduction

The importance of flow through and past porous media in technology, geo-hydrology, petroleum industry and geo-physics is indisputable. Cooling problems assume growing importance in the development of high speed vehicles. It is well known that part of the power which is necessary to overcome the drag of a space vehicle is converted into heat by internal friction within the boundary layer which surrounds the vehicle. This heat flows partially from the air layer into the surface of the vehicle by an amount which increases rapidly with the increase of the vehicle speed. As a consequence cooling problems arise in almost every component of the space vehicle. The basis for any calculation in engineering design, the aim of which is to determine the cooling requirements, is always a determination of the convective heat transfer from the heated boundary layer into the skin of the space vehicle. Extensive literature is available on this heat transfer along surfaces of idealized shapes by calculation or by experiments. Of the many solutions proposed, transpiration cooling gives an effective method in which the affected surface is manufactured from a porous material and cold fluid is ejected through the wall to form a protective layer along the surface.

When a fluid flows between impermeable surfaces, the no-slip condition is usually valid on the boundary. But when it flows over a permeable surface the no-slip boundary condition is no longer valid on that surface since there will be a migration of fluid tangential to the boundary within the permeable surface. That is, there will be a net tangential drag due to the transfer of forward momentum across the permeable interface. The velocity inside the permeable material will be different from the velocity of the fluid in the channel and we have to match the two velocities at the interface.

Beavers & Joseph¹ have experimentally investigated the effect of the tangential velocity on the Poiseuille flow over a permeable block where the upper wall is impermeable and stationary. They have shown that the mass flow rate is greatly enhanced over the value it would have attained if the block were impermeable, indicating the presence of a boundary layer in the permeable block. They have also shown that within this boundary layer the velocity at the permeable interface is greater than Darcy velocity. Rajasekhara *et al.*² have studied the effect of slip velocity on plane Couette flow taking the lower block to be a permeable surface and the upper block an impermeable surface moving with a uniform velocity u_0 . Saffman³, Taylor⁴ and Rajasekhara⁵ have investigated flow past horizontal porous beds. Rudraiah & Veerabhadraiah⁶ have evaluated the temperature distribution by considering the incompressible viscous fluid through a two-dimensional parallel channel by an impermeable moving upper plate $y = h$ and the interface $y = 0$ for the permeable material whereas Vidyanidhi *et al.*⁷ considered the same with stationary upper plate.

This paper makes a different attempt. It studies the velocity and temperature distributions in the viscous incompressible slightly conducting fluid past a permeable bed in three different configurations namely, Couette, Poiseuille and free surface flows, under the influence of uniform transverse magnetic field. To discuss the solution, the flow region is divided into two zones. In Zone 1, the flow is laminar and is governed by the Navier-Stokes equations from the impermeable upper rigid plate to the permeable bed. In Zone 2, the flow is governed by the Darcy law in the permeable bed below the nominal surface. We have evaluated the velocity distributions, the mass flow rates, the fractional increase in mass flow rates through the MHD flows with a permeable bed over what it would be if the flows were ordinary MHD flows with the impermeable lower boundary, temperature distributions and the rates of heat transfer. We have investigated the effects of magnetic parameter, porosity parameter and the Biot number on the physical quantities mentioned above. A flow configuration is shown in Fig. 1.

2. Formulation and Solution of the Problem

Zone 1: Couette Flow

We consider the flow of a viscous incompressible, slightly conducting fluid between a plate moving with velocity u_0^* and a permeable bed at a depth h under the influence

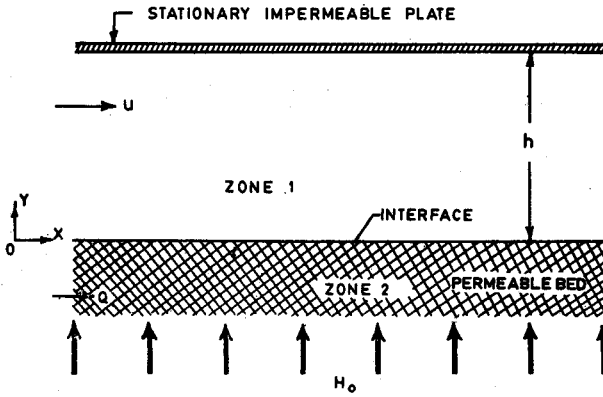


Figure 1. Flow configuration.

of a uniform transverse magnetic field. The interface is taken as the x -axis and a line perpendicular to that as the y -axis. The fluid being slightly conducting, the magnetic Reynolds number is much less than unity so that the induced magnetic field can be neglected in comparison with the applied magnetic field (Sparrow & Cess⁸).

In the absence of any input electric field, the equations governing the motion and the equation of energy are :

$$\left. \begin{aligned} \frac{\partial \bar{q}}{\partial t} + (\bar{q} \cdot \nabla) \bar{q} &= - \frac{1}{\rho} \nabla p + \nu \nabla^2 \bar{q} + \frac{\mu_e}{\rho} (\bar{J} \times \bar{H}) \\ \bar{J} &= \sigma \mu_e (\bar{q} \times \bar{H}) \end{aligned} \right\} \quad (1)$$

$$(\bar{q} \cdot \nabla) C_p T = - \frac{P}{\rho} (\nabla \cdot \bar{q}) + \nu (\nabla \cdot \bar{q})^2 + \frac{K_T}{\rho} \nabla^2 T + \frac{\bar{J}^2}{\rho \sigma} \quad (2)$$

and the continuity equation is

$$\nabla \cdot \bar{q} = 0. \quad (3)$$

where \bar{q} is the velocity of the fluid, ρ the fluid density, P the pressure, ν the kinematic coefficient of viscosity, μ_e the magnetic permeability, \bar{J} the current density, σ the electrical conductivity, \bar{H} the applied magnetic field, T the temperature, C_p the specific heat at constant pressure and K_T the thermal conductivity of the fluid. The last term in Eqn. (2) is due to Joule's dissipation. The flow is steady in the x -direction due to a constant pressure gradient $\frac{\partial p}{\partial x}$ and u is the component of the velocity in the x -direction. Now the Eqns. (1) to (3) reduce to

$$\frac{\partial^2 u}{\partial Y^2} - \frac{\sigma u^2 H_0^2}{\mu} u = \frac{1}{\mu} \frac{\partial p}{\partial x} \quad (4)$$

$$\frac{\partial^2 T}{\partial y^2} = - \frac{\mu}{K_T} \left(\frac{\partial u}{\partial y} \right)^2 - \frac{\sigma u^2 H_0^2}{K_T} u^2 \quad (5)$$

and
$$\frac{\partial u}{\partial x} = 0 \quad (6)$$

Further, $\frac{\partial}{\partial x} () = 0$, since the plate and the interface are infinitely long.

The boundary conditions are :

$$u = u_0^* \text{ at } y = h \quad (7a)$$

$$\left[\frac{\partial u}{\partial y} \right]_{y=0} = \frac{\alpha}{\sqrt{K}} (u_B - Q) \text{ (Beavers \& Joseph}^1 \text{ condition)} \quad (7b)$$

$$T = T_1 \text{ at } y = h \quad (7c)$$

$$\left[\frac{\partial T}{\partial y} \right]_{y=0} = \frac{\beta}{\sqrt{K}} (T_B^1 - T_0) \quad (7d)$$

where $Q = - \frac{K}{\mu} \frac{\partial p}{\partial x}$, α is the slip parameter (1), u_B the slip velocity, β the Biot number, T_B^1 the slip temperature, T_0 the ambient temperature and K the porosity of the material.

We introduce the following non-dimensional quantities :

$$u^* = \frac{u}{U}, u_i^* = \frac{u_0^*}{U}, y^* = \frac{y}{h}, p^* = \frac{p}{\rho U^2}, x^* = \frac{x}{h}$$

and
$$T^* = \frac{T - T_0}{T_1 - T_0} \quad (8)$$

where U is the characteristic velocity.

In view of Eqn. (8), the Eqns. (4) and (5) become (after dropping the superscripts *),

$$\frac{d^2 u}{dy^2} - Mu = -P \quad (9)$$

and
$$\frac{d^2 T}{dy^2} = -P_r E \left[\left(\frac{du}{dy} \right)^2 + Mu^2 \right] \quad (10)$$

where

$$M = \frac{\sigma \mu_e^2 H_0^2 h^2}{\mu} \text{ (Magnetic parameter)}$$

$$P = -R \frac{dp}{dx}$$

$$R = \frac{Uh}{\nu}$$

$$P_r = \frac{U^2}{C_p (T_1 - T_0)} \text{ (Prandtl number)}$$

and

$$E = \frac{\mu C_p}{K_r} \text{ (Eckert number)}$$

The non-dimensional boundary conditions are :

$$u = u_i \text{ at } y = 1 \quad (11a)$$

$$\left[\frac{du}{dy} \right]_{y=0} = \alpha_a \left(u_B - \frac{P}{a^2} \right) \quad (11b)$$

$$T = 1 \text{ at } y = 1 \quad (11c)$$

and
$$\left[\frac{dT}{dy} \right]_{y=0} = \beta a T_B \quad (11d)$$

where
$$T_B = \frac{T_B^1 - T_0}{T_1 - T_0} \text{ and } a = \frac{h}{\sqrt{K}} \text{ (Porosity parameter)}$$

Solving the Eqn. (9) using the boundary conditions (11a) and (11b), we obtain the velocity distribution

$$u = \frac{P}{M} + \frac{1}{\cos \sqrt{M}} \left[\left(u_i - \frac{P}{M} \right) \cosh (\sqrt{M} y) - \frac{\alpha a}{\sqrt{M}} \left(u_B - \frac{P}{a^2} \right) \sinh \{ \sqrt{M} (1 - y) \} \right] \quad (12)$$

where

$$u_B = \frac{aM u_i - Pa (1 - \cosh \sqrt{M}) + Pa \sqrt{M} \sinh \sqrt{M}}{a\sqrt{M} (\sqrt{M} \cosh \sqrt{M} + \alpha \sinh \sqrt{M})} \quad (13)$$

Mass flow rate : The non-dimensional mass flow rate F , per unit width of the channel is

$$\begin{aligned} F &= \int_0^1 u dy \\ &= \{ \{ \sqrt{M} \sinh \sqrt{M} - \alpha \alpha (1 - \cosh \sqrt{M}) \} aMu_i \\ &\quad + P \{ a \sqrt{M} (\alpha^* - 1) \sinh \sqrt{M} \\ &\quad + (Ma + M\alpha - 2a^2\alpha) \cosh \sqrt{M} + \alpha (2a^2 - M) \} \\ &\quad \div aM^{3/2} \{ \sqrt{M} \cosh \sqrt{M} + \alpha \sinh \sqrt{M} \} \end{aligned} \quad (14)$$

To study the effect of the porous boundary we compare this mass flow rate with the mass flow rate when the permeable boundary is replaced by an impermeable one.

If F_0^* denotes the dimensionless mass flow rate per unit width when the permeable boundary is replaced by an impermeable one, we have

$$F_0^* = \frac{(Mu_i - 2P) (\cosh \sqrt{M} - 1) + P \sqrt{M} \sinh \sqrt{M}}{M^{3/2} \sinh \sqrt{M}} \quad (15)$$

In the non-magnetic case it is found to be equal to $\frac{u_i}{2} + \frac{P}{12}$ which agrees with the result of Rajasekhara *et al.*²

Temperature distribution : Using the boundary conditions (11c) and (11d) and solving the Eqn. (10), we get the temperature distribution

$$\begin{aligned}
 T = & 1 - \beta a T_B (1 - y) + \frac{P_r E P^2 (1 - y^2)}{2M} + \frac{P_r E}{4M \cosh^2 \sqrt{M}} \\
 & \times [A^2 M (\cosh 2\sqrt{M} - \cosh 2\sqrt{M} y) \\
 & + B^2 \alpha^2 a^2 \{(1 - \cosh 2\sqrt{M} (1 - y))\} \\
 & + 2AB\alpha a \sqrt{M} \{\sinh \sqrt{M} + \sinh \sqrt{M} (1 - 2y)\}] \\
 & - \frac{P_r E B \alpha a}{M \cosh \sqrt{M}} \left[AM - B\alpha a \sqrt{M} \sinh \sqrt{M} + 2P \right. \\
 & \times \left. \cosh \sqrt{M} \right] (1 - y) + \frac{2P_r E P}{M^{3/2} \cosh \sqrt{M}} \\
 & \times [A\sqrt{M} (\cosh \sqrt{M} - \cosh \sqrt{M} y) + B\alpha a \sinh \{\sqrt{M} (1 - y)\}] \quad (16)
 \end{aligned}$$

where

$$\begin{aligned}
 T_B = & \frac{1}{1 + \beta a} + \frac{P_r E P^2}{2M (1 + \beta a)} \\
 & + \frac{P_r B}{2M (1 + \beta a) \cosh^2 \sqrt{M}} [(A^2 M - B^2 \alpha^2 a^2) \sinh^2 \sqrt{M} \\
 & + 2AB\alpha a \sqrt{M} \sinh \sqrt{M}] \\
 & - \frac{P_r E B \alpha a}{M (1 + \beta a) \cosh \sqrt{M}} [AM - B\alpha a \sqrt{M} \sinh \sqrt{M} \\
 & + 2P \cosh \sqrt{M}] + \frac{2P_r E P}{(1 + \beta a) M^{3/2} \cosh \sqrt{M}} \\
 & \times [A\sqrt{M} (\cosh \sqrt{M} - 1) + B\alpha a \sinh \sqrt{M}] \quad (17)
 \end{aligned}$$

$$A = u_i - \frac{P}{M}$$

and

$$B = u_B - \frac{P}{a^2}$$

Rate of heat transfer : From the point of view of applications in technology it is of interest to know the rates of heat transfer q between the fluid and the nominal surface and q^* between the upper plate and the fluid.

From Eqn. (15) we get

$$q = \left[\frac{dT}{dy} \right]_{y=0} = \beta a T_B \quad (18)$$

and

$$\begin{aligned} q^* &= \left[\frac{dT}{dy} \right]_{y=1} \\ &= \beta a T_B - \frac{P_r E}{M \cosh \sqrt{M}} [(P^2 + A^2 M^{3/2} - 2PBa\alpha) \cosh \sqrt{M} \\ &\quad + (B^2 a^2 \alpha^2 + 2PA) \sqrt{M} \sinh \sqrt{M} + 2PBa\alpha]. \end{aligned} \quad (19)$$

Zone 1 : Poiseuille Flow

In this part we consider the flow of a viscous incompressible, slightly conducting fluid between a stationary upper plate and a permeable bed at a distance h below the plate, under the influence of a uniform transverse magnetic field. All the results can be obtained from those of Zone 1: Couette Flow by taking $u_i = 0$.

The velocity distribution is

$$\begin{aligned} u_0 &= \frac{1}{M \cosh \sqrt{M}} [P (\cosh \sqrt{M} - \cosh \sqrt{M} y) \\ &\quad - \alpha a B_0 \sqrt{M} \sinh \{\sqrt{M} (1 - y)\}] \end{aligned} \quad (20)$$

where

$$u_{B_0} = \frac{P [\alpha \sqrt{M} \sinh \sqrt{M} - a (1 - \cosh \sqrt{M})]}{a \sqrt{M} (\sqrt{M} \cosh \sqrt{M} + \alpha a \sinh \sqrt{M})} \quad (21)$$

and

$$B_0 = u_{B_0} - \frac{P}{a^2}$$

Mass flow rate : The non-dimensional flow rate F_0 per unit width of the channel is given by

$$\begin{aligned} F_0 &= P [a\sqrt{M} (\alpha a - 1) \sinh \sqrt{M} + \{M (a + \alpha) - 2a^2\alpha\} \cosh \sqrt{M} \\ &\quad + \alpha (2a^2 - M) \div a M^{3/2} (\sqrt{M} \cosh \sqrt{M} + \alpha a \sinh \sqrt{M})] \end{aligned} \quad (22)$$

The non-dimensional mass flow rate $F_{0_0}^*$ per unit width of the channel, when the permeable boundary is replaced by an impermeable one, is given by

$$F_{00}^* = \frac{P [\sqrt{M} \sinh \sqrt{M} - 2 (\cosh \sqrt{M} - 1)]}{M^{3/2} \sinh \sqrt{M}}$$

In the non-magnetic case it takes the value $\frac{P}{12}$ which again coincides with the corresponding result of Rajasekhara *et al.*².

Temperature distribution : The temperature distribution is

$$\begin{aligned} T_0^* = & 1 - \beta a T_{B_0}^* (1 - y) + \frac{P_r E P^2 (1 - y^2)}{2M} \\ & + \frac{P_r E}{4M^2 \cosh^2 \sqrt{M}} [B_0^2 \alpha^2 a^2 M \{1 - \cosh 2\sqrt{M} (1 - y)\}] \\ & + P^2 (\cosh 2\sqrt{M} - \cosh 2\sqrt{M} y) - 2B_0 P a \alpha \sqrt{M} \{\sinh \sqrt{M} \\ & + \sinh \sqrt{M} (1 - 2y)\} + 8B_0 P a \alpha \sqrt{M} \cosh \sqrt{M} \sinh \sqrt{M} (1 - y) \\ & - 8P^2 \cosh \sqrt{M} (\cosh \sqrt{M} - \cosh \sqrt{M} y) \\ & + \frac{B_0 P_r E a \alpha (1 - y)}{M \cosh \sqrt{M}} [B_0 a \alpha \sqrt{M} \sinh \sqrt{M} \\ & + P (1 - 2 \cosh \sqrt{M})] \end{aligned} \quad (23)$$

where the slip temperature $T_{B_0}^*$ is given by

$$\begin{aligned} T_{B_0}^* = & \frac{1}{1 + \beta a} + \frac{P_r E P^2}{2M (1 + \beta a)} + \frac{P_r E}{4M^2 (1 + \beta a) \cosh^2 \sqrt{M}} \\ & \times [(B_0^2 \alpha^2 a^2 M - P^2) (1 - \cosh 2\sqrt{M}) \\ & + 4B_0 P a \alpha \sqrt{M} (\sinh 2\sqrt{M} - \sinh \sqrt{M}) \\ & - 8P^2 \cosh \sqrt{M} (\cosh \sqrt{M} - 1)] \\ & + \frac{B_0 P_r E a \alpha}{M (1 + \beta a) \cosh \sqrt{M}} [B_0 a \alpha \sqrt{M} \sinh \sqrt{M} \\ & + P (1 - 2 \cosh \sqrt{M})] \end{aligned} \quad (24)$$

Rate of heat transfer : The rates of heat transfer q_0 and q_0^* at the interface and upper boundary are given by

$$q_0 = \beta a T_{B_0}^* \quad (25)$$

and

$$\begin{aligned} q_0^* = & \beta a T_{B_0}^* - \frac{P_r E}{M^{3/2} \cosh \sqrt{M}} [\{P^2 (\sqrt{M} + 1) \\ & - 2B_0 P a \alpha \sqrt{M}\} \cosh \sqrt{M} + \{B_0^2 \alpha^2 a^2 M - 2P^2\} \sinh \sqrt{M} \\ & + 2B_0 P a \alpha \sqrt{M}] \end{aligned} \quad (26)$$

Zone 1 : Free Surface Flow

In this part, the flow of an incompressible viscous and slightly conducting fluid past a porous bed at a depth h from the free surface is considered.

The equations of momentum and energy governing the flow are respectively (9) and (10) with u and T replaced respectively by u_f and T_f , where u_f and T_f represent respectively the velocity and the temperature fields in the flow.

The relevant non-dimensional boundary conditions are

$$\frac{du_f}{dy} = 0 \text{ at } y = 1 \quad (27a)$$

$$\frac{du_f}{dy} = \alpha a \left(u_{Bf} - \frac{P}{a^2} \right) \text{ at } y = 0 \quad (27b)$$

$$T_f = 1 \text{ at } y = 1 \quad (27c)$$

and
$$\frac{dT_f}{dy} = \beta a T_{Bf} \text{ at } y = 0 \quad (27d)$$

where u_{Bf} and T_{Bf} are respectively the slip velocity and slip temperature in the present case.

Using the boundary conditions (27a) and (27b) and solving Eqn. (9) (with u replaced by u_f) we obtain the velocity distribution

$$u_f = \frac{P \sinh \sqrt{M} - B_f \alpha a \sqrt{M} \cosh \sqrt{M} (1 - y)}{M \sinh \sqrt{M}} \quad (28)$$

where

$$u_{Bf} = \frac{P (a \sinh \sqrt{M} + \alpha \sqrt{M} \cosh \sqrt{M})}{a \sqrt{M} (\sqrt{M} \sinh \sqrt{M} + \alpha \cosh \sqrt{M})} \quad (29)$$

and

$$B_f = u_{Bf} - \frac{P}{a^2}$$

Mass flow rate : The non-dimensional mass flow rate F_f per unit width of the channel is given by

$$F_f = \frac{P [(\alpha M + aM - a^2 \alpha) \sinh \sqrt{M} + a^2 \alpha \sqrt{M} \cosh \sqrt{M}]}{aM^{3/2} (\sqrt{M} \sinh \sqrt{M} + \alpha \cosh \sqrt{M})} \quad (30)$$

The non-dimensional mass flow rate $F_{f_0}^*$ per unit width of the channel, when the permeable boundary is replaced by an impermeable one, is given by

$$F_{f_0}^* = \frac{P [\sqrt{M} \cosh \sqrt{M} - \sinh \sqrt{M}]}{M^{3/2} \cosh \sqrt{M}} \quad (31)$$

In the non-magnetic case this reduces to $\frac{P}{3}$ which is four times the corresponding value in ordinary Poiseuille flow.

Temperature distribution : Using the boundary conditions (27c) and (27d) and solving Eqn. (10) (with T replaced by T_f) we get the temperature distribution

$$\begin{aligned}
 T_f = & 1 - \beta a T_{Bf} (1 - y) \\
 & + \frac{P_r E}{4M^{3/2} \sinh^2 \sqrt{M}} [2P^2 \sqrt{M} (1 - y^2) \sinh^2 \sqrt{M} \\
 & + B_f^2 \alpha^2 a^2 \sqrt{M} \{1 - \cosh 2\sqrt{M} (1 - y)\} \\
 & - 8B_f P \alpha a \sinh \sqrt{M} \{1 - \cosh \sqrt{M} (1 - y)\}] \\
 & - \frac{B_f P_r E \alpha a (1 - y)}{M \sinh \sqrt{M}} [2P \sinh \sqrt{M} \\
 & - B_f \alpha a \sqrt{M} \cosh \sqrt{M}]
 \end{aligned} \tag{32}$$

where

$$\begin{aligned}
 T_{Bf} = & \frac{1}{1 + \beta a} + \frac{P_r E}{2(1 + \beta a) M^{3/2} \sinh \sqrt{M}} [P^2 \sqrt{M} \sinh \sqrt{M} \\
 & - 2B_f P \alpha a \{2\sqrt{M} \sinh \sqrt{M} - (B_f M \alpha a + 2) \cosh \sqrt{M} + 2\}]
 \end{aligned} \tag{33}$$

Rate of heat transfer : The rate of heat transfer q_f , at the nominal surface, is given by

$$q_f = \beta a T_{Bf} - 2P_r E B_f^2 \alpha^2 a^2 M^{-1/2} \coth \sqrt{M} \tag{34}$$

Fractional increase : To make a comparative study of the mass flow rates in all the three flows considered and to find the effects of the porous boundary on these mass flow rates we have evaluated the following fractional increases in the mass flow rates :

(i) To study the effect of moving upper plate on the mass flow rate, we have calculated ϕ_0 . This is the fractional increase in mass flow rate through the plane Couette flow over what it would be if the flow were Poiseuillean, and this ϕ_0 is given by

$$\begin{aligned}
 \phi_0 = & \frac{F - F_0}{F_0} \\
 = & r a M \{ \sqrt{M} \sinh \sqrt{M} + \alpha \alpha (\cosh \sqrt{M} - 1) \} \\
 & \div [a \sqrt{M} (\alpha \alpha - 1) \sinh \sqrt{M} \\
 & + \{ M (a + \alpha) - 2a^2 \alpha \} \cosh \sqrt{M} + \alpha (2a^2 - M)]
 \end{aligned} \tag{35}$$

where

$$r = \frac{u_1}{P}$$

It is found that this quantity ϕ_0 becomes independent of α and takes the value

$$\frac{rM}{\sqrt{M} \coth \sqrt{M} - 1} \quad \text{when} \quad a^2 = \frac{M}{1 - \sqrt{M} \operatorname{cosech} \sqrt{M}}$$

In the non-magnetic case it is observed that ϕ_0 becomes independent of α and takes the value $3r$ when $a = \sqrt{6}$ which agree with the results of Rajasekhara *et al*². This phenomenon occurs when the velocity at the permeable wall of the channel is equal to the Darcy value within the permeable material.

(ii) To examine the effect of the porous boundary on the mass flow rate through plane Couette flow, we have evaluated ϕ_0^* . This is the fractional increase in the mass flow rate through MHD Couette flow with a permeable bed over what it would be if the permeable bed is replaced by an impermeable one and is given by

$$\begin{aligned} \phi_0^* &= \frac{F - F_0^*}{F_0^*} \\ &= \sqrt{M} (\cosh \sqrt{M} - 1) [aMr + \sqrt{M} \alpha \sinh \sqrt{M} \\ &\quad + a (\cosh \sqrt{M} - 1)] \div [a (\sqrt{M} \cosh \sqrt{M} + a \alpha \sinh \sqrt{M}) \\ &\quad \{ (rM - 2) (\cosh \sqrt{M} - 1) + \sqrt{M} \sinh \sqrt{M} \}] \end{aligned} \quad (36)$$

This is found to be independent of α and it takes the value

$$\frac{(\cosh \sqrt{M} - 1) (rM - 1 + \cosh \sqrt{M})}{\cosh \sqrt{M} [(rM - 2) (\cosh \sqrt{M} - 1) + \sqrt{M} \sinh \sqrt{M}]}$$

when
$$a^2_M = \frac{M \cosh \sqrt{M}}{rM - 1 + \cosh \sqrt{M}}$$

In the limiting case as $M \rightarrow 0$, the above quantity is seen to take the value $(3 + 6r) \div (1 + 6r)$ and this is attained when $a_0^2 = \frac{2}{1 + 2r}$ which agrees with the result of Rajasekhara *et al*². It can be noted that this occurs when the velocity profile has a zero gradient at the permeable wall.

Rajasekhara *et al*² have observed that the rectilinear flow in the channel breaks down under certain conditions when $a_0^2 > \{ 2 \div (1 + 2r) \}$ because the average size of the individual pores within the material becomes at least equal to the channel width. However, since a^2_M is greater than a_0^2 for small M , such a breakdown of rectilinear flow may be prevented when the average size of the pore is not too large.

(iii) In order to study the impact of the porous boundary on the mass flow rate through MHD plane Poiseuille flow, ϕ_0^* is computed. ϕ_0^* denotes the fractional

increase in the mass flow rate through MHD Poiseuille flow with a permeable bed over what it would be if the flow were ordinary MHD Poiseuille flow and is given by

$$\begin{aligned} \phi_{00}^* &= \frac{F_0 - F_{00}^*}{F_{00}^*} \\ &= \sqrt{M} (\cosh \sqrt{M} - 1) [\sqrt{M} \alpha \sinh \sqrt{M} + a (\cosh \sqrt{M} - 1)] \\ &\quad \div [a (\sqrt{M} \cosh \sqrt{M} + a \alpha \sinh \sqrt{M}) \{ \sqrt{M} \sinh \sqrt{M} \\ &\quad - 2 \cosh \sqrt{M} + 1 \}] \end{aligned} \tag{37}$$

in the non-magnetic case this becomes $\frac{3(a + 2\alpha)}{a(1 + a\alpha)}$

which agrees with the result of Beavers & Joseph¹. The quantity ϕ_{00}^* becomes independent of α and takes the value

$$\frac{(\cosh \sqrt{M} - 1)^2}{\cosh \sqrt{M} (\sqrt{M} \sinh \sqrt{M} - 2 \cosh \sqrt{M} + 2)}$$

when $a^2 = \frac{M \cosh \sqrt{M}}{\cosh \sqrt{M} - 1}$.

In the non-magnetic case this fractional increase becomes independent of α and takes the value 3 when $a = \sqrt{2}$. This result again coincides with the one obtained by Beavers & Joseph¹.

(iv) With a view to observe the effect of the porosity of the lower boundary in the free surface flow, we have evaluated ϕ_{f0}^* which denotes the fractional increase in the mass flow rate through MHD free surface flow with permeable bed over it would be if the flow were ordinary MHD free surface flow. This ϕ_{f0}^* is given by

$$\begin{aligned} \phi_{f0}^* &= \frac{F_f - F_{f0}^*}{F_{f0}^*} \\ &= \frac{\sqrt{M} \sinh \sqrt{M} (\alpha M \cosh \sqrt{M} + a \sinh \sqrt{M})}{a (a\alpha \cosh \sqrt{M} + \sqrt{M} \sinh \sqrt{M}) (\sqrt{M} \cosh \sqrt{M} - \sinh \sqrt{M})} \end{aligned} \tag{38}$$

In the non-magnetic case this reduces to $\frac{3(a + \alpha)}{a^2\alpha}$

The quantity ϕ_{f0}^* becomes independent of α and takes the value

$$\frac{\sinh \sqrt{M}}{(\sqrt{M} \cosh \sqrt{M} - \sinh \sqrt{M})} \quad \text{when } a = \sqrt{M}. \text{ In the non-magnetic case}$$

$\phi_{f_0}^*$ becomes independent of α and tends to infinity when a tends to zero. Therefore, if $\phi_{f_0}^*$ in the non-magnetic case is to be independent of α we have noticed that the mass flow rate $F_{f_0}^*$ tends to zero when a tends to zero.

It is interesting to note that, in the non-magnetic case, the relevant fractional increases are $3r$ in the case of Couette flow and 3 in the case of Poiseuille flow while it tends to infinity in the case of free surface flow.

We have studied the effects of the magnetic parameter M , the slip parameter α and the porosity parameter a on all the physical quantities obtained. The effects of PrE (the product of Prandtl and Eckert numbers) and the Biot number β on the slip temperature, temperature distribution and the rates of heat transfer coefficients have also been studied. The behaviours of the various quantities are depicted in Figs. 2 to 10.

3. Conclusions

Conclusions were drawn on the basis of numerical work and figures.

Slip Velocity

It is observed that the slip velocities decrease with the increase in the magnetic parameter. The slip velocity in the free surface flow decreases more rapidly than that in the Couette flow which in turn decreases more rapidly than that in the Poiseuille flow. This change in rapidities is clearly visible for small values of M . It is seen that the slip velocities in the three flows increase with the increase in α whereas they decrease with the increase in a . We have also observed from Fig. 2 that for any given set of values of the parameters the slip velocity is greatest in the case of Couette flow and least in the case of Poiseuille flow.

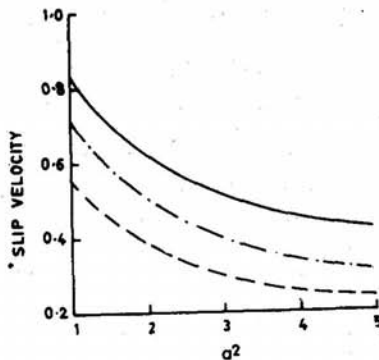


Figure 2. Slip velocity plotted against the porosity parameter.

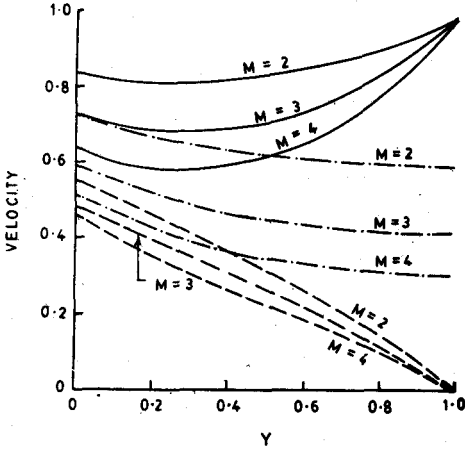


Figure 3. Velocity profiles for different values of the magnetic parameter.

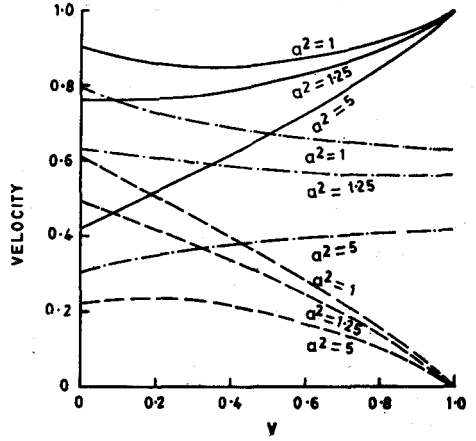


Figure 4. Velocity profiles for different values of the porosity parameter.

Velocity Distribution

We have observed that the velocities in the three flows decrease with the increase in M , throughout the flow field (Fig. 3). In the case of Couette flow we have noticed that the velocity first decreases and then increases with the increase in y while the velocities in the other two flows decrease with the increase in y . It is seen that the velocities in the cases of Poiseuille and free surface flows decrease with the increase in y for all values of α . The decrease in the case of Poiseuille flow is found to be more rapid than that in the case of free surface flow. In the case of Couette flow the velocity first decreases and then increases with the increase in y . Fig. 4 shows that the velocity in the case of Poiseuille flow first increases and then decreases with the increase in y for sufficiently large values of α , whereas it decreases with the increase in y for smaller values of α . In the case of free surface flow, the velocity increases with the increase in y for sufficiently large values of α whereas it decreases with the increase in y for smaller values of α . In the case of Couette flow, the velocity first decreases and then increases with the increase in y for sufficiently small values of α , whereas it increases with the increase in y for larger values of α . We have seen that velocities in all the three flows increase with the increase in α whereas they decrease with the increase in α throughout the flow field. We have also observed that for any given set of values of the parameters, the velocity at any given point of the flow field is maximum in the case of Couette flow and minimum in the case of free surface flow.

Mass Flow Rate

We have noticed that the mass flow rates in the three flows decrease as the magnetic parameter increases. The decrease in the case of free surface flow is more

rapid than that in either of the other two flows. This rapidity is clearly visible for smaller values of M . It is seen that the mass flow rates in all the three flows increase with α for sufficiently small a while they decrease with the increase in α for larger values of a . We have noticed that the mass flow rates in all the three flows decrease with the increase in a . We have also observed the fact that the mass flow rate is maximum in the case of Couette flow and least in the case of Poiseuille flow.

Fractional Increases

We have noticed that ϕ_0 alone increases with M while the others decrease as shown in Fig. 5. We have observed that ϕ_0 decreases with the increase in α for all values for a . But the others increase with α for sufficiently small values of a and decrease for larger values of a . We have also observed that ϕ_0 increases with the increase in a while ϕ_0^* , ϕ_{00}^* and ϕ_{f0}^* decrease with the increase in a for all value of α .

Slip Temperature

We have observed that the slip temperature increases in the case of Couette flow, first increases and then decreases in the case of Poiseuille flow and decreases in the

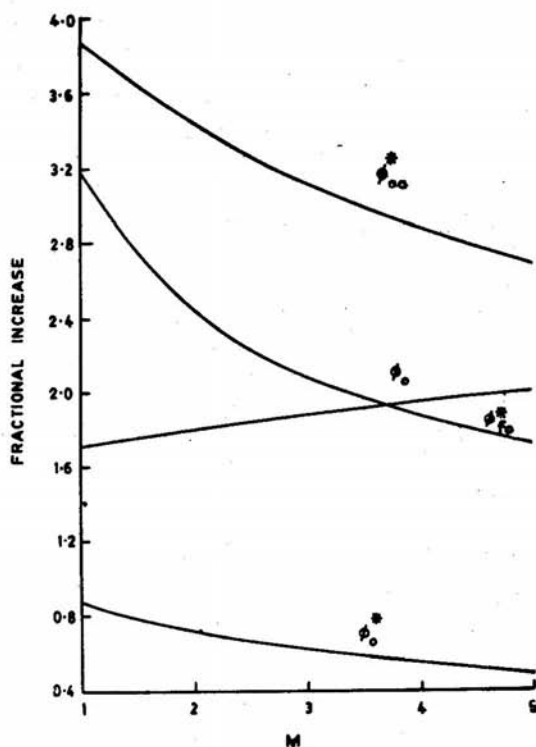


Figure 5. Fractional increase against magnetic parameter.

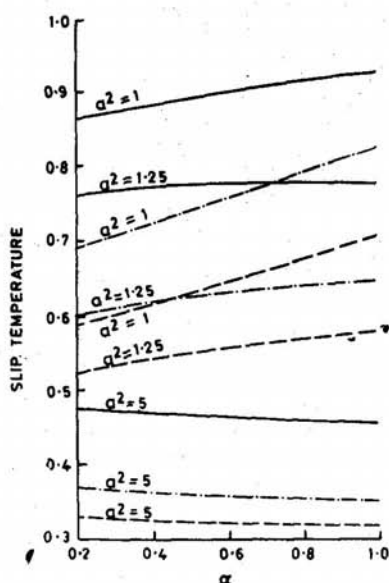


Figure 6. Slip temperature against α for different values of a .

case of free surface flow with the increase in M . For small M the increase in the case of Couette flow is more rapid than in the case of Poiseuille flow. We have seen that the slip temperatures increase with the increase in the product of Prandtl and Eckert numbers. From Fig 6, we have noticed that the slip temperatures in all the flows increase with α for sufficiently small values of a while they decrease for larger values of a . We have also observed that the slip velocities gradually increase with the increase in α for all values of the Biot number β . We have seen that the slip temperature decreases with the increase in a or β for all values of α . We have also found that for a given set of values for the parameters, the slip temperature is maximum in the case of Couette flow and maximum in the case of Poiseuille flow.

Temperature Distribution

We have noticed from Fig. 7 that the temperature increases with the increase in M in the case of Couette flow while it decreases as M increases in the case of free surface flow. At any point of the flow field this increment is seen to be greater than the corresponding decrement in the temperature of the free surface flow. But in the case of Poiseuille flow we have observed that the temperature distribution is not uniform, in that it is neither increasing throughout the field nor decreasing throughout. In fact, if we consider two temperatures of this flow corresponding to two different values of M then we find that the one with smaller M is smaller than the other

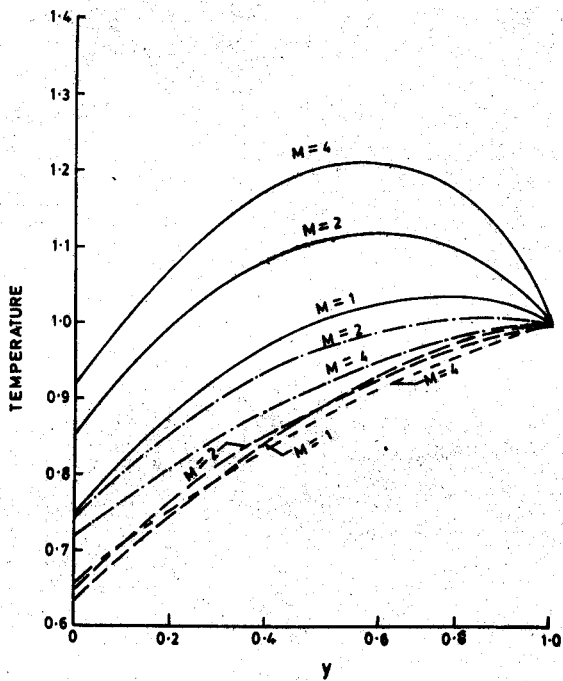


Figure 7. Temperature profiles for different values of the magnetic parameter.

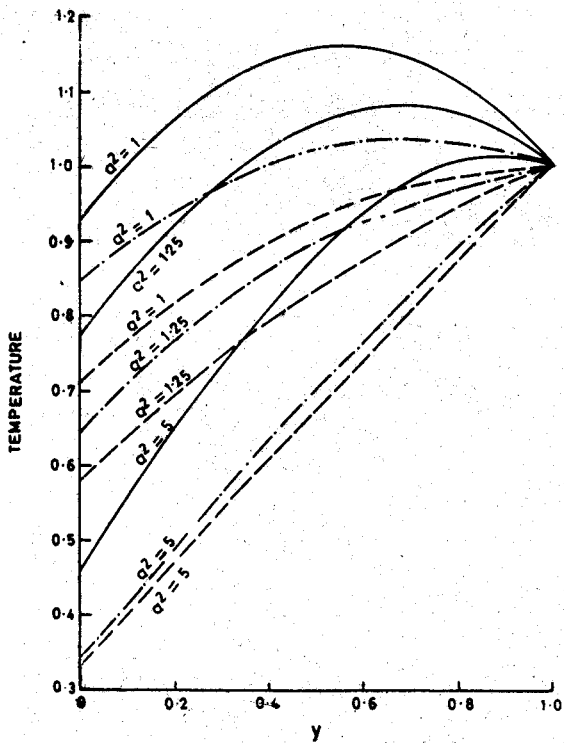


Figure 8. Temperature profiles for different values of porosity parameter.

at points sufficiently close to the nominal surface. This trend, however, gets reversed and the temperature decreases as M increases at points sufficiently away from the interface. In the case of Couette flow the temperature increases sharply and then decreases with the increase in y for all values of M . In the case of Poiseuille flow the temperature increases with the increase in y for all values of M . But in the case of free surface flow the temperature first increases and then decreases with the increase in y for small values of M and increases with y for larger values of M . We have observed that the temperature profiles of the three flows are linear and coincident for $P_r E = 0$. We have also seen that the temperatures increase with the increase in $P_r E$, the increase being maximum in the case of Couette flow and least in the case of Poiseuille flow at all points of the flow field. We have noticed that the temperatures increase with the increase in the slip parameter α . It is seen from Fig. 8 that the temperatures decrease with the increase in a . It can also be seen that in each flow this fall in temperature increases with the increase in a at all points of the flow field. We have observed that the temperatures decrease with the increase in β in all the three flows. It can also be noticed that in any flow the decrease in the temperature decreases as β increases.

We have also found that at any point of the flow field the temperature is greatest in the case of Couette flow and least in the case of Poiseuille flow.

The Rates of Heat Transfer

We have observed that q and q_0^* increase with M while q_f and q^* decrease as shown in Fig. 9. But to start with q_0 increases with M and then gradually decreases as M increases. We have found that q , q_0 and q_f increase with the increase in $P_r E$, whereas q^* and q_0^* decrease. We have also noticed that q^* decreases very fast with the increase in $P_r E$. We have seen from Fig. 10 that the non-uniform nature of q_f as α increases for different values of a . We have also noticed that q and q_0 decrease with the increase in α for sufficiently large values of a whereas they increase for smaller values of a . It is seen that q , q_0 and q_f increase with the increase in a or β .

Zone 2 : Couette Flow

The flow region is the permeable bed immediately below the nominal surface. The flow in this region is governed by the Darcy law.

The equations governing motion are

$$Q = -\frac{K}{\mu} \left(\frac{\partial p}{\partial x} \right) \quad (39)$$

$$\frac{\partial^2 u}{\partial y^2} - \frac{u}{K} = \frac{1}{\mu} \left(\frac{\partial P}{\partial x} \right) + \frac{\sigma \mu_0^2 H_0^2 u}{\mu} \quad (40)$$

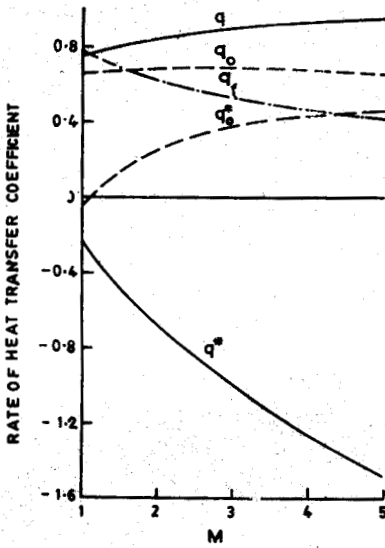


Figure 9. Heat transfer coefficient plotted against the magnetic parameter.

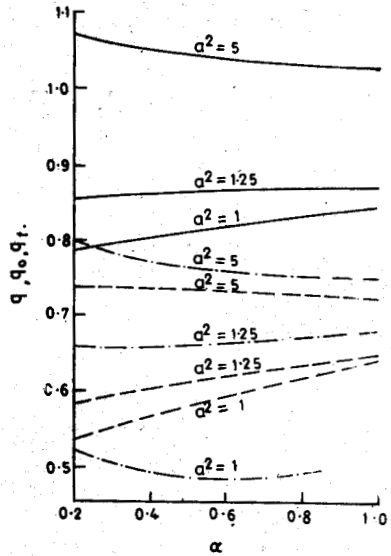


Figure 10. Heat transfer coefficient at the interface against α for different values of a .

$$K_T \frac{\partial^2 T}{\partial y^2} + \mu \left(\frac{\partial u}{\partial y} \right)^2 + \frac{\mu}{K} u^2 + \sigma \mu_e^2 H_0^2 u^2 = 0 \tag{41}$$

where u and T are now the velocity and temperature distributions in Zone 2. The boundary conditions are

$$u = U u_B \text{ at } y = 0 \tag{42a}$$

$$u = Q \text{ (finite) at } y = -\delta \tag{42b}$$

$$T = T_B^1 \text{ at } y = 0 \tag{42c}$$

$$T = T_0 \text{ at } y = -\delta \tag{42d}$$

where δ is the boundary layer thickness just below the nominal surface. We assume that this thickness is the same for both the velocity and temperature distributions.

In view of the non-dimensional quantities given in Eqn. (8), Eqns. (39) to (42) reduce to

$$\frac{d^2 u}{dy^2} - b^2 u = -P \tag{43}$$

$$\frac{d^2 T}{dy^2} = -P_r E \left[\left(\frac{du}{dy} \right)^2 + b^2 u^4 \right] \tag{44}$$

$$u = u_B \text{ at } y = 0 \tag{45a}$$

$$u = \frac{P}{a^2} \text{ at } y = \frac{-\delta}{h} = -\delta^* \quad (45b)$$

$$T = T_B = \frac{T_B^1 - T_0}{T_1 - T_0} \text{ at } y = 0 \quad (45c)$$

$$T = 0 \text{ at } y = -\delta^* \quad (45d)$$

after dropping the superscripts '*' and taking $b^2 = a^2 + M$.

Using the conditions (45) and solving the Eqns. (43) and (44) we obtain the velocity and temperature distributions

$$u = [B^* a^2 b^2 \sinh b (\delta^* + y) + P a^2 \sinh b \delta^* - MP \sinh by] \div a^2 b^2 \sinh b \delta^* \quad (46)$$

and

$$\begin{aligned} T = & \left(\frac{\delta^* + y}{\delta^*} \right) T_B + \frac{P_r E}{4a^4 b^4 \sinh^2 b \delta^*} [B^{*2} \{ \cosh 2b \delta^* \\ & - \cosh 2b (\delta^* + y) \} + M P^2 (1 - \cosh 2by) \\ & - 2B^* a^2 b^2 M P \{ \cosh b \delta^* - \cosh b (\delta^* + 2y) \} \\ & - 2P a^2 b^2 y^2 \sinh^2 b \delta^* \\ & + 8a^2 M P^2 \sinh b \delta^* \sinh b y \\ & + 8B^* a^2 b^2 P \sinh b \delta^* \{ \sinh b \delta^* - \sinh b (\delta^* + y) \}] \\ & + \frac{P_r E y}{2a^4 b^4} [B^{*2} a^4 b^4 - M P^2 - a^4 b^2 P^2 \delta^{*2} \\ & + 4B^* a^4 b^4 P - 4a^2 M P^2] \quad (47) \end{aligned}$$

where

$$B^* = u_B - \frac{P}{b^2}$$

Expression for the boundary layer thickness : We know that, at the edge of the boundary layer, the shear stress has to be zero. In other words

$$\frac{du}{dy} = 0 \text{ at } y = -\delta^*$$

Therefore the expression for δ^* is given by

$$\delta^* = \left[\frac{2 (B^* a^2 b^2 - M P)}{M P b^2} \right]^{1/2} \quad (48)$$

neglecting the terms of $O(\delta^{*4})$

Zone 2 : Poiseuille Flow

The velocity and temperature distributions and the expression for the thickness of the boundary layer are obtained from those of the Couette flow by taking u_i to be zero. Thus Eqns. (46) to (48) give the velocity, temperature and the thickness of the boundary layer respectively for this flow. B^* , T_B and δ^* are respectively replaced by B_0^* , T_{B0} and δ_0^* where $B_0^* = u_{B0} - \frac{P}{b^2}$ and δ_0^* is the boundary layer thickness in the flow under consideration.

Zone 2 : Free Surface Flow

The non-dimensional equation governing the flow and the energy equation are (43) and (44). The relevant non-dimensional boundary conditions are

$$u = u_{Bf} \text{ at } y = 0 \quad (49a)$$

$$u = \frac{P}{a^2} \text{ at } y = -\frac{\delta_f}{h} = -\delta_f^* \quad (49b)$$

$$T = T_{Bf} = \frac{T_{Bf}^1 - T_0}{T_1 - T_0} \text{ at } y = 0 \quad (49c)$$

$$\text{and } T = 0 \text{ at } y = -\delta_f^* \quad (49d)$$

The governing equations and the boundary conditions suggest that the velocity, temperature and the thickness of the boundary layer corresponding to this flow are respectively given by (46), (47) and (48) by replacing B^* , T_B and δ^* respectively by B_f^* , T_{Bf} and δ_f^* where $B_f^* = u_{Bf} - \frac{P}{b^2}$ and δ_f^* is the non-dimensional thickness of the boundary layer in the present case.

Acknowledgement

The first author (RVG) is thankful to University Grants Commission, India for granting him fellowship under Faculty Improvement Programme.

References

1. Beavers, G. S. & Joseph, D. D., *J. Fluid Mech.*, 30 (1967), 197,
2. Rajasekhara, B. M., Rudraiah, N. & Ramaiah, B. K., *Journal of Mathematical & Physical Sciences*, 9 (1975), 49.

3. Saffman, P. G., *Stud. Appl. Math.*, **50** (1971), 93.
4. Taylor, G. I., *J. Fluid Mech.*, **49** (1971), 319.
5. Rajasekhara, B. M., Experimental and Theoretical Study of Flow Past Porous Media, Ph.D. Thesis, Bangalore University, 1974.
6. Rudraiah, N. & Veerabhadraiah, R., *Proc. Indian Acad. Sci.*, **86A** (1977), 537.
7. Vidyanidhi, V., Sithapati, A. & Narayana, P. C. L., *Proc. Ind. Acad. Sci.*, **86A** (1977), 557.
8. Sparrow, E. M. & Cess, R. D., *Trans. ASME., J. Appl. Mech.*, **29** (1962), 181.